

Antiferromagnetic polarization in the periodic Anderson lattice

G. Z. Wei and H. Q. Nie

Department of Physics, Northeast University of Technology, Shenyang, People's Republic of China

(Received 29 April 1991)

By using a third-order approximation of the local approach to the periodic symmetric Anderson lattice, the ground-state energy, the correlation energy, the local magnetic moment, and the antiferromagnetic polarization are obtained. We found that the local magnetic moment and the antiferromagnetic polarization increase with increasing one-site f - f electronic Coulomb interaction U and with decreasing d - f electronic hybridization strength V .

Extensive experimental and theoretical studies have been made on the heavy-fermion compounds and their alloys since their discovery. Very different characteristics have been found experimentally for various cerium compounds at low temperature. For example, CeCu_2Si_2 is a superconductor,¹ while CeB_6 and CeAl_2 are magnetically ordered. CeCu_6 is a normal Fermi liquid even at 8 mK. For different values of the alloy composition y , CeSi_{2-y} and $\text{CeNi}_y\text{Pt}_{1-y}$ may be either nonmagnetic or magnetically ordered.^{2,3} These interesting and anomalous properties are related to the spin fluctuations of 4f electrons. In a theoretical analysis of these properties, the periodic Anderson model is commonly used. Many techniques have been used to solve periodic-Anderson-lattice problems, such as functional integration⁴, the real-space renormalization-group method,⁵ the Gutzwiller variational approach,⁶⁻⁸ large-orbital-degeneracy N^{-1} expansions,⁹ and Monte Carlo techniques.^{10,11}

The local approach, which has been developed from the Gutzwiller variational method,^{12,13} has successfully been used to describe correlations between the d electrons of the transition metals.^{14,15} Except for the third-order calculation on a six-atom Hubbard model ring by Horsch¹⁶ and our works on both the Hubbard and extended Hubbard model,^{17,18} all of the existing works using the local approach are within the scope of the second-order approximation. Horsch discovered that, for the Hubbard model, the correction of the correlation energy E_c of the third-order approximation is not negligibly small compared with that in the second order; our early works have reached the same conclusion when considering the local operator $O = n_{i\uparrow}n_{i\downarrow}$. We believe that results obtained with the third-order approximation are more reliable than those of second order, and conclude that the f -electron correlations also have a local nature. Therefore, we use the local approach to investigate correlation effects of the Anderson lattice up to the third-order approximation. In this paper, we assume a paramagnetic ground state for a not so large value of U (Ref. 19) and study the antiferromagnetic polarization in the periodic Anderson simple-cubic lattice.

The nondegenerate periodic-Anderson-lattice Hamiltonian is written as

$$H = H_1 + H_2 + H_3 + H_4, \quad (1)$$

where

$$\begin{aligned} H_1 &= \sum_{k,\sigma} \epsilon_k d_{k\sigma}^\dagger d_{k\sigma}, \\ H_2 &= \epsilon_{f0} \sum_{i,\sigma} f_{i\sigma}^\dagger f_{i\sigma}, \\ H_3 &= \frac{V}{\sqrt{N}} \sum_{i,k,\sigma} (e^{ik \cdot \mathbf{R}_i} f_{i\sigma}^\dagger d_{k\sigma} + \text{H.c.}), \\ H_4 &= \frac{U}{2} \sum_{i,\sigma} f_{i\sigma}^\dagger f_{i\sigma} f_{i-\sigma}^\dagger f_{i-\sigma}, \end{aligned}$$

in the symmetric half-filled case

$$\epsilon_{f0} + U/2 = \epsilon_F = 0, \quad N_e/N = 2, \quad (2)$$

where $d_{k\sigma}^\dagger$ ($d_{k\sigma}$) is creation (annihilation) operator for a d electron with momentum k and spin σ , $f_{i\sigma}^\dagger$ ($f_{i\sigma}$) is creation (annihilation) operator for a localized nondegenerate f orbital (i denotes the site) with energy ϵ_{f0} , U is the Coulomb repulsion between electrons with opposite spins in the f orbital and describes a short-range interaction between them. V is the positive hybridization parameter of d - f electrons in the same site, N_e and N are the total number of electrons and sites, respectively, and the number of d and f electrons, n_d and n_f , per site are $n_d = n_f = 1$.

Within the local approach, one first decomposes the Hartree-Fock ground state $|\Psi_{\text{HF}}\rangle$ into a near combination of configurations. The trial function for the correlation ground state $|\Psi_L\rangle$ is constructed by modulating the linear combination as

$$|\Psi_L\rangle = \prod_{ij} \left[\prod_m (1 - \eta_m O_{ij}^{(m)}) \right] |\Psi_{\text{HF}}\rangle, \quad (3)$$

where $\{\eta_m\}$ is a set of variational parameters, the indices i and j run over all sites, and $\{O_{ij}^{(m)}\}$ is a set of local operators. For simplicity we only consider the single-site correlations, then, $O_{ij}^{(m)}$ reduces to $O = n_{i\uparrow}n_{i\downarrow}$, and η_m to η . For a given local operator, the ground-state energy is written as

$$E_G = \frac{1}{N} \frac{\langle \Psi_L | H | \Psi_L \rangle}{\langle \Psi_L | \Psi_L \rangle} = E_{\text{HF}} + E_C. \quad (4)$$

The first term of (4) is the HF ground-state energy, the

second term of (4) is the correlation energy, and the parameter η is determined by minimization of the ground-state energy E_G . The ground-state energy E_G is related to the correlation function. We use the Green's-function technique developed by Zubarev.²⁰ The Green's functions are defined as

$$\begin{aligned} G_{ij}^{\sigma\sigma'} &= \langle\langle f_{i\sigma}; f_{j\sigma'}^\dagger \rangle\rangle_\omega, & F_{ik}^{\sigma\sigma'} &= \langle\langle f_{i\sigma}; d_{k\sigma'}^\dagger \rangle\rangle_\omega, \\ K_{kj}^{\sigma\sigma'} &= \langle\langle d_{k\sigma}; f_{j\sigma'}^\dagger \rangle\rangle_\omega, & D_{kk'}^{\sigma\sigma'} &= \langle\langle d_{k\sigma}; d_{k'\sigma'}^\dagger \rangle\rangle_\omega. \end{aligned} \quad (5)$$

One can solve the equation of motion with decoupling procedures and obtain the correlation functions in the Hartree-Fock ground state

$$\begin{aligned} \langle d_{k\sigma}^\dagger d_{k\sigma} \rangle &= \frac{\omega^-}{\omega^- - \omega^+}, \\ \langle d_{k\sigma}^\dagger f_{i\sigma} \rangle &= \frac{1}{\sqrt{N}} e^{ik \cdot R_i} \frac{V}{\omega^- - \omega^+}, \\ \omega^\pm &= \frac{1}{2}(\epsilon_k \pm \sqrt{\epsilon_k^2 + 4V^2}). \end{aligned} \quad (6)$$

A systematic scheme has been formulated to calculate E_C as a power series of η . When $0 \leq \eta < 1$, the series expansion is effective. Up to the third order in η the correlation energy can be expressed as

$$\tilde{E}_C = -2\eta A + \eta^2 B - \frac{1}{3}\eta^3 C, \quad (7)$$

where η satisfies the following equation due to $\partial E_G / \partial \eta = 0$:

$$C\eta^2 - 2B\eta + 2A = 0.$$

The coefficients of η in (7) are calculated with Wick's theorem and the linked-diagram rule (the diagram used in Fig. 1) are as follows:

$$A = \langle 0H \rangle_{\text{HF}} = 22\tilde{U}a^4, \quad (8)$$

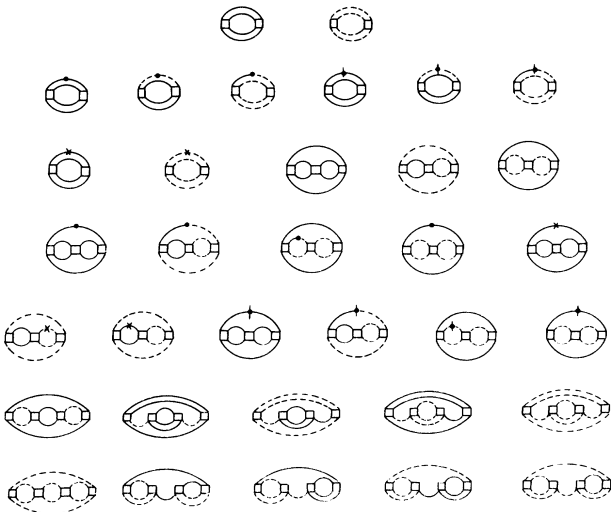


FIG. 1. Schematic representation of diagrams which contribute to A , B , and C , where \times represents $d_k^\dagger d_k$; \bullet represents $f_i^\dagger f_i$; \blacklozenge represents $f_i^\dagger d_k$; \square represents $n_{i\uparrow} n_{i\downarrow}$; the lines correspond to elements of the density matrix: solid lines for diagonal elements and dashed lines for nondiagonal elements.

$$B = \langle 0H0 \rangle_{\text{HF}} + \langle 00H \rangle_{\text{HF}} = -2a^2(7\tilde{E}_1 + 3\tilde{E}_2), \quad (9)$$

$$C = 3\langle 00H0 \rangle_{\text{HF}} + \langle 000H \rangle_{\text{HF}} = -306\tilde{U}a^7, \quad (10)$$

where A corresponds to the first row, B to the second and third rows, and C to the others in Fig. 1. a , \tilde{E}_1 , and \tilde{E}_2 in Eqs. (8)–(10) are as follows:

$$\begin{aligned} a &= \frac{1}{4}, \\ \tilde{E}_1 &= 2\tilde{V}^2 \ln \left[\frac{1 + \sqrt{1 + 16\tilde{V}^2}}{4\tilde{V}} \right], \\ \tilde{E}_2 &= -4\tilde{V}^2 + 16\tilde{V}^3 \arctan(1/4\tilde{V}). \end{aligned}$$

In order to provide explicit results quantitatively, we have taken the rectangular density of states, and E_C has been defined as normalized energy $\tilde{E}_C = E_C/W$ as a function of $\tilde{U} = U/W$ and $\tilde{V} = V/W$, where W is the bandwidth. The normalized ground-state energy \tilde{E}_G is given as

$$\tilde{E}_G = E_G/W = \tilde{E}_{\text{HF}} + \tilde{E}_C,$$

where

$$\tilde{E}_{\text{HF}} = -\frac{1}{4}\sqrt{1 + 16\tilde{V}^2} + 2\tilde{E}_1 - \frac{\tilde{U}}{4}. \quad (11)$$

Computation results of the correlation energy per site \tilde{E}_C vs Coulomb interaction \tilde{U} are shown in Fig. 2 and the correlation ground-state energy \tilde{E}_G vs Coulomb interaction \tilde{U} is shown in Fig. 3. The curves a , b , c , d , and e in Figs. 2 and 3 correspond, respectively, to $\tilde{V} = 0.5, 0.4, 0.3, 0.2$, and 0.1 . We found that, for constant \tilde{V} , \tilde{E}_C decreases with increasing \tilde{U} . For constant \tilde{U} , \tilde{E}_C increases with increasing \tilde{V} , while the correlated ground-state energy \tilde{E}_G increases with increasing \tilde{V} for constant \tilde{U} . This indicates that the paramagnetic phase would become unstable if \tilde{V} becomes smaller and smaller for fixed \tilde{U} . The local magnetic moments of f electrons are defined as

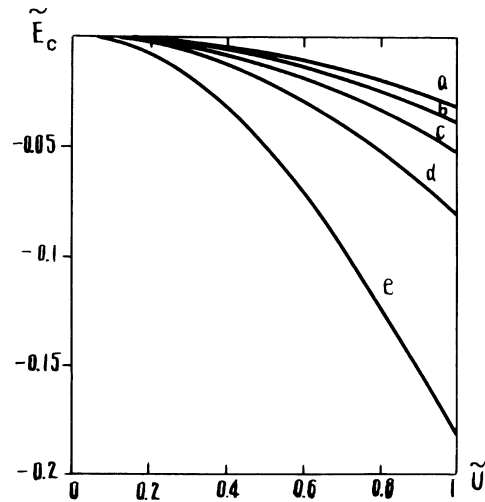


FIG. 2. Correlation energy \tilde{E}_C vs Coulomb interaction \tilde{U} . The curves a , b , c , d , and e correspond, respectively, to fixed $\tilde{V} = 0.5, 0.4, 0.3, 0.2$, and 0.1 .

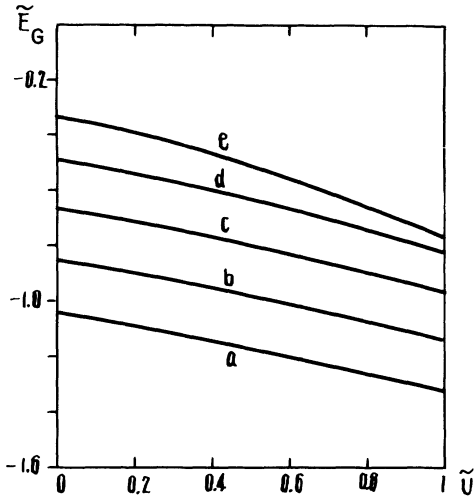


FIG. 3. Ground-state energy \tilde{E}_G vs \tilde{U} for the same \tilde{V} as in Fig. 2.

$\langle S_i^2 \rangle$ and are related to the correlation function $\langle n_{i\uparrow} n_{i\downarrow} \rangle$ by writing the spin operators in terms of fermion operators:

$$S_m = \langle \Psi_L | S_i^2 | \Psi_L \rangle = \frac{3}{4}(n_f - 2\langle n_{i\uparrow} n_{i\downarrow} \rangle), \quad (12)$$

where

$$\langle n_{i\uparrow} n_{i\downarrow} \rangle = \frac{1}{4} - 2\eta A_1 + \eta^2 B_1 - \frac{1}{3}\eta^3 C_1 \quad (13)$$

for the third-order-approximation calculation. The calculation procedure of A_1 , B_1 , and C_1 are similar to those of A , B , and C .

The curves of the local magnetic moments S_m vs \tilde{U} for the same as in Fig. 2 are plotted in Fig. 4. For fixed \tilde{V} , the local magnetic moments decrease with decreasing \tilde{U} . This decrease in the local magnetic moment reflects the transition from localization to nonlocalization for f electrons. From the results of the present work, it can be seen that with increasing pressure, \tilde{U} decreases due to the

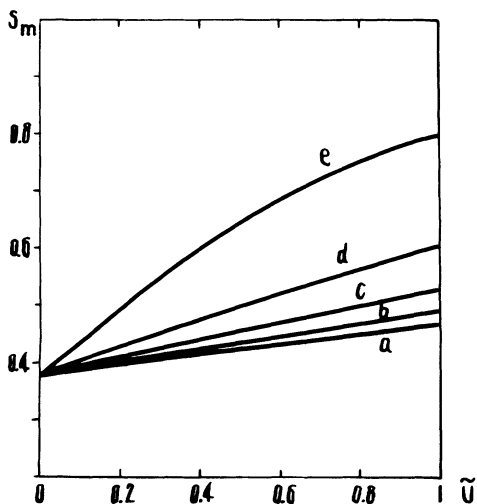


FIG. 4. Local moments S_m vs \tilde{U} for the same \tilde{V} as in Fig. 2.

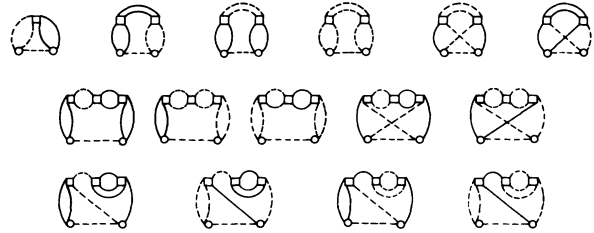


FIG. 5. Schematic representation of diagrams which contribute to A_2 , B_2 , and C_2 , where $\circ \cdots \circ$ represents $n_i n_j$. Other symbols are the same as in Fig. 1.

bandwidth W becoming larger, so that the local magnetic moments of f electrons decrease. This is consistent with the valence changes in the cerium compounds.

The discussions about the paramagnetic phase of the Anderson lattice are relevant to the problem of polarization induced by the local magnetic moments. Although the long-range order disappears, a short-range order may still exist. The polarization is defined as

$$P_L = \langle \Psi_L | n_{1\sigma} n_{2-\sigma} | \Psi_L \rangle - \langle \Psi_L | n_{1\sigma} n_{2\sigma} | \Psi_L \rangle. \quad (14)$$

If P_L is greater than the corresponding Hartree-Fock value, we will call the polarization antiferromagnetic; otherwise, it is called ferromagnetic. In the third-order approximation, the expression of P_L may be written as

$$P_L = a - 2\eta A_2 + \eta^2 B_2 - \frac{1}{3}\eta^3 C_2, \quad (15)$$

where A_2 , B_2 and C_2 are calculated with the diagrams shown in Fig. 5. We obtained

$$\begin{aligned} A_2 &= -2a^3, \\ B_2 &= a^3(4 - 2a + a^2), \\ C_2 &= -3a^4(9 - 11a - 2a^2). \end{aligned} \quad (16)$$

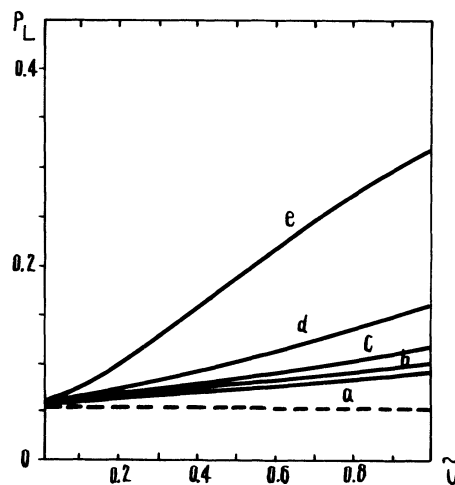


FIG. 6. Antiferromagnetic polarization P_L vs \tilde{U} for the same \tilde{V} as Fig. 2, where the dotted curve represents the Hartree-Fock polarization.

The calculated local polarization is shown in Fig. 6, where Hartree-Fock local polarization is indicated by the dotted curve. We see that the local polarization is always antiferromagnetic. For a fixed \tilde{U} , the antiferromagnetic polarization increases with decreasing \tilde{V} ; for a fixed \tilde{V} , the antiferromagnetic polarization increases with increasing \tilde{U} . This change of the antiferromagnetic polarization with \tilde{U} or \tilde{V} is similar to the change of the local magnetic moments. The mechanism of the antiferromagnetic polarization is then not difficult to understand. Let us assume that a site is occupied by one f electron with up spin. The larger the \tilde{U} , the easier any f electron with down spin will be pushed from this site to its neighbors. Then a localized magnetic moment occurs by which the antiferromagnetic polarization is induced. On the other hand, when $\tilde{V} \neq 0$, conduction electrons hop on and off

the f orbital to mix these two f electron spin states. The larger the \tilde{V} , the easier is the mixture and the smaller the localized magnetic moments. The competition of these two processes described above would lead to the antiferromagnetic polarization in the paramagnetic phase. This conclusion is qualitatively consistent with results of Monte Carlo simulations.¹¹

In conclusion, by using a third-order approximation of the local approach to a periodic symmetric Anderson lattice, the ground-state energy, the correlation energy, the local magnetic moment, and the antiferromagnetic polarization have been calculated in the present work. We found that the local magnetic moment and the antiferromagnetic polarization increase with increasing one-site f - f electronic Coulomb interaction U and with decreasing d - f electronic hybridization strength V .

¹F. Steglich *et al.*, Phys. Rev. Lett. **43**, 1892 (1979).

²H. Yashima and J. Satoh, Solid State Commun. **41**, 723 (1982).

³D. Gignoux and J. C. Gomonex-Sal, Phys. Rev. B **30**, 3967 (1984).

⁴P. Coleman, J. Magn. Magn. Mater. **47&48**, 323 (1985).

⁵R. Julien and R. M. Martin, Phys. Rev. B **26**, 8173 (1982).

⁶B. H. Brandow, Phys. Rev. B **33**, 215 (1986).

⁷T. M. Rice and K. Ueda, Phys. Rev. Lett. **55**, 995 (1985).

⁸C. M. Varma, W. Weber, and L. J. Randall, Phys. Rev. B **33**, 1015 (1986).

⁹N. Read, D. M. Nems, and S. Doniach, Phys. Rev. B **30**, 3841 (1984).

¹⁰D. Kung *et al.*, Phys. Rev. B **32**, 2022 (1984).

¹¹R. Blankenbecler *et al.*, Phys. Rev. Lett. **58**, 411 (1987).

¹²G. Stollhoff and P. Fulde, Z. Phys. B **26**, 257 (1977).

¹³G. Stollhoff and P. Fulde, Z. Phys. B **29**, 231 (1978).

¹⁴A. M. Oleś, Phys. Rev. B **28**, 327 (1983).

¹⁵A. M. Oleś, *et al.*, Phys. Lett. **102A**, 323 (1984).

¹⁶P. Horsh, Z. Phys. B **33**, 43 (1979).

¹⁷G. Z. Wei *et al.*, Phys. Lett. A **120**, 353 (1987).

¹⁸G. Z. Wei *et al.*, Int. J. Mod. Phys. B **1**, 1311 (1987).

¹⁹K. Yamada and K. Yosida, J. Magn. Magn. Mater. **33-34**, 461 (1983).

²⁰D. N. Zubarev, Usp. Fiz. Nauk. **71**, 71 (1960).